Nanoscale Res Lett (2009) 4:748–752
DOI 10.1007/s11671-009-9309-7

NANO EXPRESS

Intense Red Catho- and Photoluminescence from 200 nm Thick Samarium Doped Amorphous AlN Thin Films

Muhammad Maqbool · Tariq Ali

Received: 21 January 2009 / Accepted: 2 April 2009 / Published online: 25 April 2009

Abstract Samarium (Sm) doped aluminum nitride (AlN) thin films are deposited on silicon (100) substrates at 77 K by rf magnetron sputtering method. Thick films of 200 nm are grown at 100–200 watts RF power and 5–8 m Torr nitrogen, using a metal target of Al with Sm. X-ray diffraction results show that films are amorphous. Cathodoluminescence (CL) studies are performed and four peaks are observed in Sm at 564, 600, 648, and 707 nm as a result of $^4G_{5/2} \rightarrow {}^6H_{5/2}$, $^4G_{5/2} \rightarrow {}^6H_{7/2}$, $^4G_{5/2} \rightarrow {}^6H_{9/2}$, and $^4G_{5/2} \rightarrow {}^6H_{11/2}$ transitions. Photoluminescence (PL) provides dominant peaks at 600 and 707 nm while CL gives the intense peaks at 600 nm and 648 nm, respectively. Films are thermally activated at 1,200 K for half an hour in a nitrogen atmosphere. Thermal activation enhances the intensity of luminescence.

Keywords Cathodoluminescence · Photoluminescence · Thermal activation · XRD · Samarium · AlN

Introduction

Rear-earth doped nitride semiconductors thin films are attracting increasing attention as phosphor materials, and are used for optical displays [1–5]. Sputter deposited AlN has been shown to be a viable host for luminescent rare earth (RE) ions due to its transparency over a wide range, including the UV, IR, and entire visible range [6–17]. Recent progress toward nitride-based light-emitting diode and electroluminescent devices (ELDs) has been made using crystalline and amorphous AlN doped with a variety of rare-earth elements [1–9]. The electronic structure of the RE ions differ from the other elements and are characterized by an incompletely filled $4f^n$ shell. The $4f$ electrons lay inside the ion and are shielded from the surroundings by the filled $5s^2$ and $5p^6$ electron orbital [17]. When these materials are excited by various means, intense sharp-line emission is observed due to intra-$4f^n$-shells transitions of the rare-earth ion core [18–21]. The amorphous III-nitride semiconductors have the advantage over their crystalline counterpart because the amorphous material can be grown at room temperature with little stress due to lattice mismatch [22]. They may also be more suitable for waveguides and cylindrical and spherical laser cavities because of the elimination of grain boundaries at low-temperature growth [5].

High thermal conductivity, stability, and chemical inertness of AlN also make it very useful for its electrical and thermal applications.

In the present work, luminescence properties of Samarium (Sm) are studied when deposited in AlN host. The spectra obtained provide data in a broad range from 300 to 800 nm. Thus luminescence from the films in UV, visible, and IR are obtained and studied simultaneously. The effect of thermal activation is also studied by activating these materials in a tube furnace up to 1,200 K.

Experimental Details

Thin films of amorphous AlN:Sm were prepared at 77 K by rf magnetron sputtering of an aluminum target of 99.999%

M. Maqbool (✉)
Department of Physics and Astronomy, Ball State University, Muncie, IN 47306, USA
e-mail: mmaqbool@bsu.edu

T. Ali
Department of Physics, State University of New York at Buffalo, Buffalo, NY 14260, USA

purity in a pure nitrogen atmosphere. Doping of thin films with Sm was accomplished by drilling a small hole (0.5 cm diameter) in the aluminum target (4.2 cm diameter) and placing a slug of Sm in the hole. Sm was then co-sputtered with the aluminum. The rf power was varied between 100 and 200 watts. All films were deposited onto 2 cm × 2 cm, or less, p-silicon (100) substrates. The background pressure in the chamber was $<3 \times 10^{-5}$ Torr. Liquid nitrogen was used to keep the temperature of the film at 77 K. The metallic substrate holder was designed such that it had a half inch diameter cylindrical hole from the top. The substrate was pasted on the metal base of the holder below the liquid nitrogen. Liquid nitrogen was constantly poured in the holder to provide a constant low-temperature to the substrate during film growth.

The as-deposited films were characterized for their characteristic emissions. The thickness of the films was 200 nm, measured with a quartz crystal thickness monitor in the growth chamber. X-rays diffraction (XRD) was used to determine the structure of the films. No diffraction peaks were observed, indicating that the as-deposited films were amorphous.

Cathodoluminescence (CL) studies of the films were performed at room temperature in a vacuum chamber at a pressure of about 3×10^{-6} Torr, which was maintained with an Alcatel CFF 450 turbo pump. Films were excited with electron beam energy of 2.85 kV and beam current of 100 μA. The films were placed an angle of 45° to the incident electron beam coming out of electron gun. The detector was placed at an angle of 45° to the film such that lines joining electron gun, the film and detector were making and angle of 90°. Luminescence from the films was focused onto the entrance slit of a SPEX Industries double monochromator with gratings blazed at 500 nm and detected at a Thorn EMI fast high gain photomultiplier tube with a range of 200–900 nm. The resolution of the spectra was 1 nm.

A 488 nm line of Argon laser was used to obtain the photoluminescence spectra, analyzed by a spectrometer equipped with a cooled photomultiplier tube. The power of the laser beam was 9.3 mW.

Thermal activation was accomplished by placing the flat films in a tube furnace at 1,200 K in a nitrogen atmosphere for half an hour.

Results and Discussion

Figure 1 shows the photoluminescence (PL) spectrum of AlN:Sm when excited with a 488 nm Argon laser. A strong emission occurred at 598 nm (near 600 nm) which is indicated by a sharp peak in the figure. This peak corresponds to $^4G_{5/2} \rightarrow {}^6H_{9/2}$ transition. The intensity of the emission is very strong and hence it serves as a potential candidate for a red laser production at 598 nm. Further the PL is showing that the material can emit light under photon excitation and can be optically pumped for a laser construction. This work is still in progress and will be reported once laser achievement is successful.

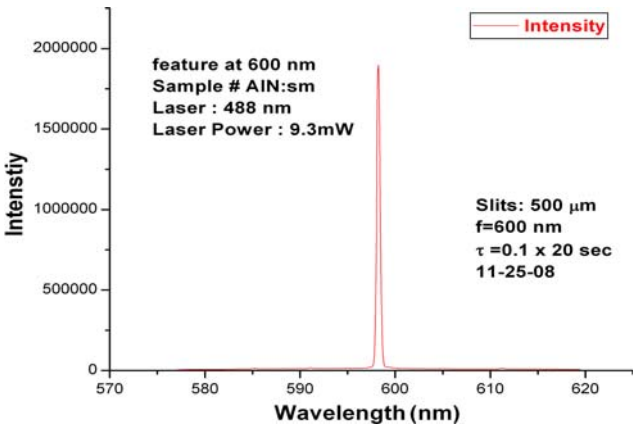

Fig. 1 PL spectrum of amorphous AlN:Sm with excitation at 488 nm and emission at 598 nm

Figure 2 shows the PL spectrum of AlN:Sm when excited with the same 488 nm Argon laser. A very strong emission occurred at 707 nm (near 710 nm) which is indicated by a sharp peak in the figure. This peak corresponds to $^4G_{5/2} \rightarrow {}^6H_{11/2}$ transition. The intensity of the emission is very strong and hence it also serves as a potential candidate for an orange-red laser production at 707 nm. The intensity of this peak is almost double than the intensity of the peak at 598 nm with the same power of excitation sourcing. Thus the $^4G_{5/2} \rightarrow {}^6H_{11/2}$ transition has a strong potential to produce a red-near IR laser under optimum conditions.

Figure 3 provides CL spectrum of AlN:Sm in 300–850 nm range at room temperature. It is observed that

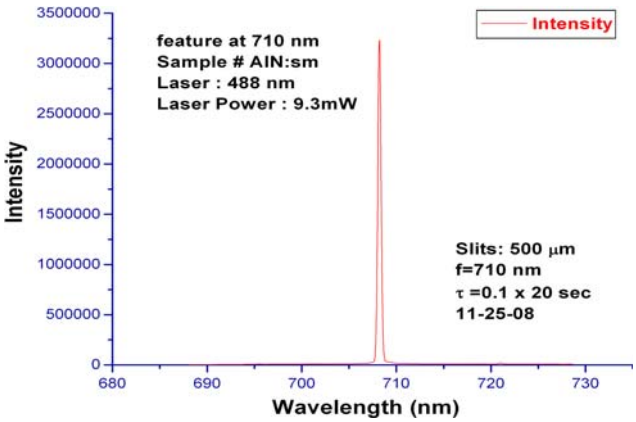

Fig. 2 PL spectrum of amorphous AlN:Sm with excitation at 488 nm and emission at 707 nm

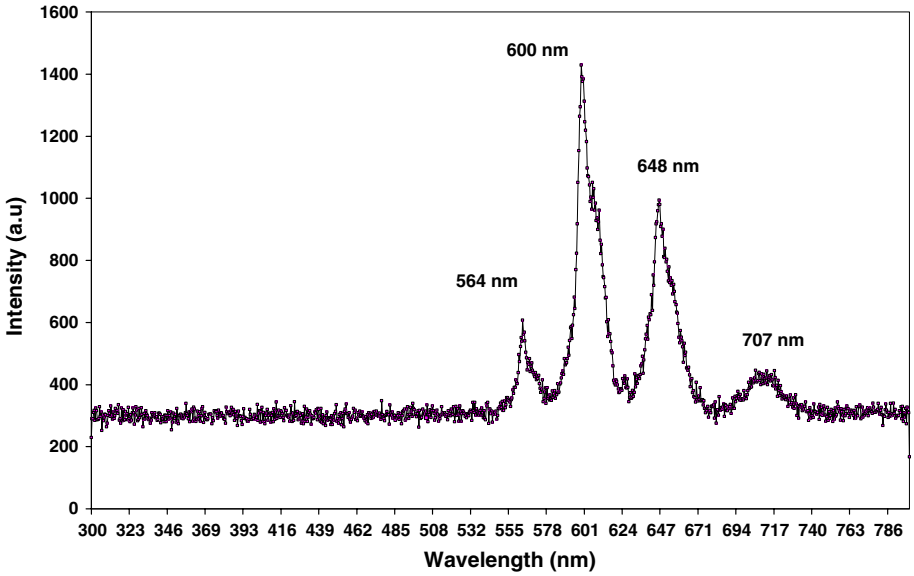

Fig. 3 CL spectrum of amorphous AlN:Sm films

Sm^{3+} give four transitions under electron excitation. Three of these transitions are in the visible range of the spectrum at 564, 600, and 648 nm as a result from $^4G_{5/2} \rightarrow {}^6H_{5/2}$, $^4G_{5/2} \rightarrow {}^6H_{7/2}$ and $^4G_{5/2} \rightarrow {}^6H_{9/2}$ transitions, respectively [7, 20]. The fourth peak falls in the infrared region at 707 nm due to $^4G_{5/2} \rightarrow {}^6H_{11/2}$. The peak at 600 nm is the strongest while the peak at 707 nm is the weakest amongst all. The $^4G_{5/2} \rightarrow {}^6H_{5/2}$ transition at 564 nm falls in yellow region of the spectrum. The dominant transition $^4G_{5/2} \rightarrow {}^6H_{7/2}$ at 600 nm and the $^4G_{5/2} \rightarrow {}^6H_{9/2}$ transitions occur in red region of the visible spectrum. Because of the combination of these colors and dominancy of orange-red peak, the direct observation of AlN:Sm films exposed to electron beam in CL gives orange-red light to naked eye. All these transitions and their relative intensities are tabulated in Table 1.

Figure 4 gives a combined spectra of AlN:Sm before and after thermal activation. It is clear from the figure that thermal annealing enhances the luminescence from Sm. It is observed that thermal annealing doubles the luminescence intensity from the dominant transition $^4G_{5/2} \rightarrow {}^6H_{7/2}$ at 600 nm. The $^4G_{5/2} \rightarrow {}^6H_{5/2}$ transition at 564 nm has got maximum enhancement when annealed thermally at 1,200 K for half an hour. The intensity of luminescence of this transition increases by a factor of 2.5 after thermal annealing. The other two transitions are also enhanced significantly by thermal annealing.

Figure 5 shows the XRD analysis of the AlN:Sm films deposited on Si(100) substrate. Only one peak can be observed in the film at 69.1° that corresponds to Si(100). No other peak is present in the figure, indicating that the deposited films are amorphous. Thermal activation of the films at 1,200 K has not changed the structure of the films.

Table 1 provides detail of all transitions from Sm^{3+}. Column 2 and 3 give all transitions and the corresponding wavelengths of emission. The relative intensities of non-annealed and annealed samples are given in column 4 and 5, respectively. These relative intensities are determined by comparing the intensity of every peak to the intensity brightest peak (567 nm) in the non-annealed samples. Column 4 gives the ratio by which the intensity of luminescence is enhanced by thermal annealing. Careful

Table 1 Summary of Sm^{3+} ions emissions from AlN:Sm

Material	Transition	Wavelength (nm)	Relative intensity non-annealed films.	Relative intensity of annealed films	Enhancement ratio
CL data					
AlN:Sm	$^4G_{5/2} \rightarrow {}^6H_{5/2}$	564	0.425	1.07	2.52
	$^4G_{5/2} \rightarrow {}^6H_{7/2}$	600	1.000	2.3	2.3
	$^4G_{5/2} \rightarrow {}^6H_{9/2}$	648	0.686	1.143	1.66
	$^4G_{5/2} \rightarrow {}^6H_{11/2}$	707	0.312	0.457	1.46
PL data					
	$^4G_{5/2} \rightarrow {}^6H_{7/2}$	598	0.61		
	$^4G_{5/2} \rightarrow {}^6H_{11/2}$	707	1.00		

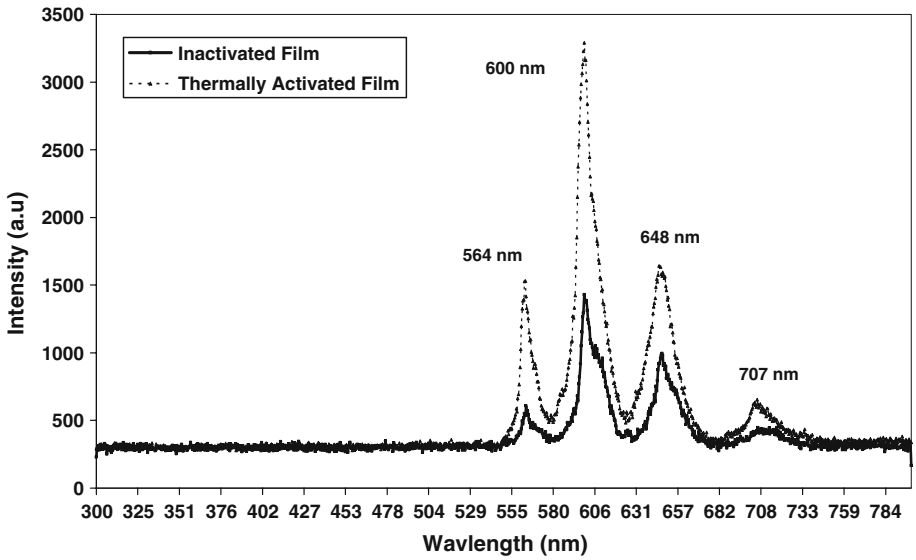

Fig. 4 CL spectra of thermally activated and inactivated amorphous AlN:Sm films

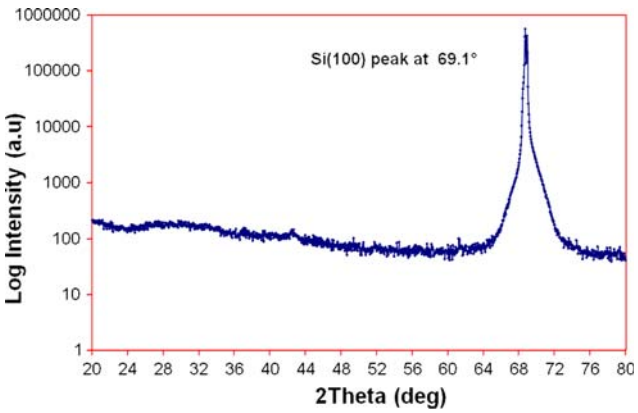

Fig. 5 XRD analysis of the AlN:Sm films deposited on Si(100) substrates

consideration of these ratios tells that enhancement is higher for lower wavelengths and it goes down when one moves from ultraviolet to infrared region of the spectrum. The reason being, with increasing temperature the probability of populating higher energy levels increases and hence higher energy levels are thermally more populated as compared to lower energy levels at high-temperature [21]. These thermally populated higher energy levels give rise to enhanced emission.

Both PL peaks indicate very strong emission from AlN:Sm when excited with 488 nm laser. Such a strong intensity clearly indicates that this material is a potential candidate for laser production. We are in the process of providing optimum conditions and laser power to achieve laser in AlN:Sm. Polarization study is also in progress and will be published soon once it is complete.

This significant increase in the intensities of luminescence from Sm^{3+} ions by thermal annealing has got a good explanation. Luminescence occurs from Sm^{3+} ions and not from Sm^{2+} or Sm^{1+}. During the film deposition, it is most likely that some of Al^{3+} of AlN may be replaced by Sm^{3+} but there are also chances for imperfections and defects giving rise to Sm^{2+} or Sm^{1+} during film growth. These ions do not contribute to luminescence. Smaller the number of these ions, more will be Sm^{3+} ions and hence luminescence will be higher. When these films are activated thermally at a higher temperature then most of Sm^{2+} or Sm^{1+} impurities ionize and converts to Sm^{3+} ions giving path to enhanced luminescence [22–24]. Moreover when the films are transferred to the furnace and thermally activated after removed from the deposition chamber, they are exposed to air. Thus oxidation of the surface of the film cannot be ignored. Oxygen enhances the luminescence of rare-earth ions giving rise to the enhanced luminescence after thermal activation of the films [13].

The results show that amorphous AlN:Sm is a promising candidate for its use in nanoscale optical devices and communication tools. The strong red emission makes this material a potential candidate for making quantum dots.

Conclusion

Thin films of amorphous AlN:Sm are deposited by rf magnetron sputtering. Films were characterized for their surface morphology and luminescence properties by XRD, PL, and CL. Samarium ion emits mainly in visible region with the most intense transition in the orange-red portion of the spectrum. Thermal activation enhances the luminescence of films. PL provides very sharp emission in red making it a useful material for nanoscale optical devices applications.

References

1. M. Maqbool, I. Ahmad, H.H. Richardson, M.E. Kordesch, Appl. Phys. Lett. **91**(19), 193511 (2007)
2. M. Maqbool, H.H. Richardson, M.E. Kordesch, J. Mater. Sci. **42**(14), 5657–5660 (2007). doi:10.1007/s10853-006-0730-3
3. M. Maqbool, I. Ahmad, Curr. Appl. Phys. **9**, 234–237 (2008). doi:10.1016/j.cap.2008.02.001
4. M. Maqbool, H.H. Richardson, M.E. Kordesch, in Materials Research Society International Symposium proceedings, vol. 831 Article E8.12.1, @2005 Materials Research Society
5. M. Maqbool, H.H. Richardson, P.G. Van Patten, M.E. Kordesch, in Materials Research Society International Symposium proceedings, vol. 798 (Materials Research Society, 2004), pp. 8.5.1–8.5.5
6. H. Chen, K. Gurumurugan, M.E. Kordesch, W.M. Jadwisienczak, H.J. Lozykowski, MRS Internet J. Nitride Semicond. Res. **5**, U130 (2000)
7. M. Caldwell, H.H. Richardson, M.E. Kordesch, MRS Internet J. Nitride Semicond. Res. **5**, U142 (2000)
8. W.M. Jadwisienczak, H.J. Lozykowski, F. Perjeru, H. Chen, M. Kordesch, I. Brown, Appl. Phys. Lett. **76**, 3376 (2000). doi:10.1063/1.126652
9. V. Dimitrova, P.G. Van Patten, H.H. Richardson, M.E. Kordesch, Appl. Phys. Lett. **77**, 478 (2000). doi:10.1063/1.127016
10. V. Dimitrova, P.G. Van Patten, H. Richardson, M.E. Kordesch, Appl. Surf. Sci. **175–176**, 481 (2001). doi:10.1016/S0169-4332(01)00128-3
11. M.L. Caldwell, A.L. Martin, C.M. Spalding, V.I. Dimitrova, P.G. Van Patten, M.E. Kordesch, H.H. Richardson, J. Vac. Sci. Technol. A **19**, 1894 (2001)
12. M.L. Caldwell, A.L. Martin, V.I. Dimitrova, P.G. Van Patten, M.E. Kordesch, H.H. Richardson, Appl. Phys. Lett. **78**, 1246 (2001). doi:10.1063/1.1351531
13. M.L. Caldwell, P.G. Van Patten, M.E. Kordesch, H.H. Richardson, MRS Internet J. Nitride Semicond. Res. **6**, 13 (2001)
14. H.H. Richardson, P.G. van Patten, D.R. Richardson, M.E. Kordesch, Appl. Phys. Lett. **80**, 2207 (2002). doi:10.1063/1.1464220
15. H. Chen, K. Chen, D.A. Drabold, M.E. Kordesch, Appl. Phys. Lett. **77**, 1117 (2000). doi:10.1063/1.1289496
16. M.E. Little, M.E. Kordesch, Appl. Phys. Lett. **78**, 2891 (2001). doi:10.1063/1.1370548
17. J.F. Suyver, P.G. Kik, T. Kimura, A. Polman, G. Franzo, S. Coffa, Nucl. Instr. Meth. Phys. Res. B **148**, 497–501 (1999)
18. J.B. Gruber, B. Zandi, H.J. Lozykowski, W.M. Jadwisienczak, J. Appl. Phys. **91**(5), 2929–2935 (2002). doi:10.1063/1.1436297
19. H.J. Lozykowski, Phys. Rev. B **48**, 17758 (1993). doi:10.1103/PhysRevB.48.17758
20. A.J. Steckl, R. Birkhahn, Appl. Phys. Lett. **73**, 1700 (1998). doi:10.1063/1.122250
21. M.J.V. Bell, L.A.O. Nunes, A.R. Zanatta, J. Appl. Phys. **86**(1), 338–341 (1999). doi:10.1063/1.370734
22. M. Overberg, C.R. Abernathy, J.D. MacKenzie, S.J. Pearton, R.G. Wilson, J.M. Zavada, Mater. Sci. Eng. B **81**, 121–126 (2001). doi:10.1016/S0921-5107(00)00686-3
23. J.D. MacKenzie, C.R. Abernathy, S.J. Pearton, U. Hommerich, J.T. Seo, R.G. Wilson, J.M. Zavada, Appl. Phys. Lett. **72**(21), 2710–2712 (1998). doi:10.1063/1.121107
24. S.Z. Wang, S.F. Yoon, L. He, X.C. Shen, J. Appl. Phys. **90**(5), 2314–2320 (2001). doi:10.1063/1.1391213